

Chapter 1

Protonated Polycyclic Aromatic Hydrocarbons and the Interstellar Medium

1.1 Interstellar Molecules

Although hydrogen is the most abundant element in the universe, it is other elements that determine the complexity of interstellar chemistry. Besides hydrogen and helium which account for 98% of the mass of a gas of ‘solar composition,’ the next most abundant elements are oxygen, carbon, and nitrogen (Table 1.1). Together with hydrogen, these elements form the main building blocks for molecules detected in the interstellar medium, or ISM.

Table 1.1: Abundance of the more common chemical elements in the solar system [4].

Element		Abundance Atoms / 10^6 Si
H	Hydrogen	$2.72 \cdot 10^{10}$
He	Helium	$2.15 \cdot 10^9$
O	Oxygen	$2.01 \cdot 10^7$
C	Carbon	$1.21 \cdot 10^7$
Ne	Neon	$3.76 \cdot 10^6$
N	Nitrogen	$2.48 \cdot 10^6$
Mg	Magnesium	$1.08 \cdot 10^6$
Si	Silicon	$1.00 \cdot 10^6$
Fe	Iron	$9.00 \cdot 10^5$
S	Sulfur	$5.15 \cdot 10^5$

Table 1.2: Identified interstellar and circumstellar molecules and molecular ions (as of Dec. 2004).

		Number of atoms								
		2	3	4	5	6	7	8	9	10+
H ₂	H ₂ O	NH ₃	CH ₄	CH ₃ OH	HCCCH ₃	CH ₃ COOH	(CH ₃) ₂ O	(CH ₃) ₂ CO		
CO	H ₂ S	H ₂ CO	SiH ₄	CH ₃ SH	HC(O)CH ₃	HC(O)OCH ₃	C ₂ H ₅ OH	C ₂ H ₅ OH		
CSi	HCN	H ₂ CS	CH ₂ NH	C ₂ H ₄	CH ₃ NH ₂	H ₃ C ₃ -CN	C ₂ H ₅ CN	C ₂ H ₅ CN		
CP	HNC	C ₂ H ₂	NH ₂ CN	HC ₄ H	CH ₂ CH(CN)	HOCH ₂ C(O)H	CH ₃ C ₄ H	CH ₃ C ₄ H		HC ₈ CN
CS	CO ₂	HNCO	CH ₂ CO	CH ₃ CN	HC ₄ -CN	C ₆ H ₂	HC ₆ CN	HC ₆ CN		
NO	SO ₂	HNCS	HCOOH	CH ₃ NC	C ₆ H	C ₆ H ₂	C ₈ H	C ₈ H		C ₆ H ₆
NS	MgCN	H ₃ O ⁺	HCC-CN	HC(O)NH ₂	c-C ₂ H ₄ O	C ₂ H ₆	C ₂ H ₆	C ₂ H ₆		OC(CH ₂ OH) ₂
SO	MgNC	HOCO ⁺	HCC-NC	HCCC(O)H	CH ₂ CH(OH)	C ₇ H	C ₇ H	C ₇ H		
HCl	NaCN	C ₃ S	c-C ₃ H ₂	C ₅ H		H ₂ CCHC(O)H				HC ₁₁ N
NaCl	N ₂ O	H ₂ CN	1-C ₃ H ₂	HC ₃ NH ⁺						
KCl	NH ₂	c-C ₃ H	CH ₂ CN	C ₅ O						
AlCl	OCS	1-C ₃ H	C ₄ H	C ₅ N						
AlF	HCO	HCCN	C ₄ Si							
PN	C ₃	H ₂ CO ⁺	C ₅							
SiN	C ₂ H	C ₂ CN	HNCCC							
SiO	HCO ⁺	C ₃ O	H ₂ COH ⁺							
SiS	HOC ⁺	HCNH ⁺								
NH	N ₂ H ⁺	CH ₂ D ⁺								
OH	HNO	CH ₃								
C ₂	HCS ⁺	SiC ₃								
CN	H ₃ ⁺	ND ₃								
HF	C ₂ O									
CO ⁺	C ₂ S									
SO ⁺	SiC ₂									
CH	AlNC									
CH ⁺	CH ₂									
SH	SiCN									
LiH										
FeO										

Nearly 150 molecules and molecular ions have been detected in interstellar and circumstellar environments to date [5,6] (Table 1.2). Most of them are small, 2 – 4 atom molecules. Many of the larger molecules are linear or highly symmetric and have large dipole moments which facilitate their detection. There must be many more less abundant or not as strongly absorbing/emitting molecules in the ISM that have not yet been detected or positively identified. One such suite of molecules involves polycyclic aromatic hydrocarbons (PAHs) and their derivatives. While PAHs are believed to be present in the ISM in large quantities, benzene is the only aromatic molecule for which a possible detection has been reported using high resolution spectroscopy such as that used to assemble Table 1.2 [7].

1.2 PAHs and the Unidentified IR Emission Bands

In 1973, an Unidentified Infrared Emission band (UIR) was observed at $11.3 \mu\text{m}$ from a planetary nebulae [8]. A few other observations of a variety of objects added 3.3, 6.2, 7.7, 8.6, 12.7, 14.2, and $16.2 \mu\text{m}$ bands to the UIR list [9–13]. The strongest emission was observed from dusty regions bathed in the intense UV radiation from nearby young stars. The emitting species could not be identified exactly, although some conclusions were made about their nature.

Associated with these UIR bands is a pseudo-continuum component whose color temperature is independent of the distance from the exciting star [14]. Thus, both the continuum and bands must be produced by the ‘heating’ associated with the absorption of a single photon [15,16]. This requires the species responsible for the emission to be intermediate in size, between small molecules and macroscopic dust grains ($\sim 20 - 50$ atoms). It has been noted that some of the vibrations of aromatic hydrocarbons are close in wavelength to many of the UIR features [17]. Based on intensity ratios and the correlation observed among different

UIRs, it has been suggested that the PAHs which generate these IR bands are peripherally hydrogenated, should have pericondensed structures, and may be ionized [16, 18].

Numerous laboratory experiments have been conducted to measure the IR and visible spectra of neutral and ionic PAHs, and the results have been compared to astronomical observations [19–21]. From laboratory measurements, it was established that both neutral and cationic PAHs may be UIR carriers [22], but that ionized PAHs provide a better match to the general characteristics observed in the interstellar spectra. Density functional calculations added protonated PAHs to that list [23]. Although no single PAH species can account for the full suite of UIR features alone, it is possible to approximate the observed astronomical spectra by a mixture of many different PAHs [24].

PAHs are believed to be ubiquitous in the ISM, for the UIR features are observed throughout the galaxy. As a class, they may be the most abundant organic species in the ISM, and may account for up to 20% of total interstellar carbon [25]. They may also be responsible for other astronomical features, such as the Diffuse Interstellar Bands, discussed next.

1.3 The Diffuse Interstellar Bands

The Diffuse Interstellar Bands, or DIBs, present the longest-standing puzzle in astronomical spectroscopy [26]. The DIBs are 1 – 200 cm^{-1} wide features in seen visible and near infrared spectra of reddened stars, produced by the absorption of star light by species in diffuse or translucent interstellar clouds. They were originally discovered in 1922 [27], but their interstellar nature was only established some twelve years later [28, 29]. By 1975, 39 DIBs had been discovered [30]. Thanks to ongoing improvements in astronomical spectrographs and especially in CCD arrays, a large number of weaker DIBs have now been

discovered. Based on more recent surveys [31–33], for example, there are more than 150 known DIBs that span the wavelength interval from 380 to 950 nm (Figure 1.1).

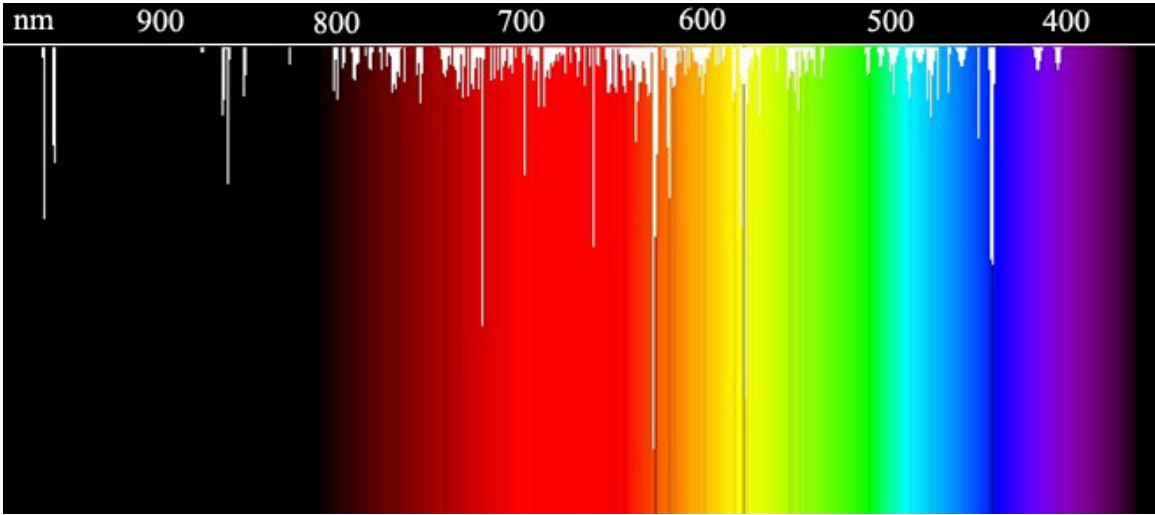


Figure 1.1: A synthetic spectrum of the diffuse interstellar bands, based on the DIB compilation in [1]. The image is from [2].

Many different theories have been proposed to account for the DIBs. The wide range of DIB widths and the fact that a few of the DIBs are seen in emission toward unusual objects points to the molecular nature of the species responsible. Carriers cannot reside on or within dust particles or grains because particle size, shape and composition influence the peak positions and profiles, which have not been observed astronomically. Since a wide variety of carbon-containing species are found in space and since the overall strength of the DIBs is well correlated with the $[C]/[H]$ ratio, carbonaceous molecules or radicals are the most attractive candidates. Among them are [34, 35]:

1. Highly unsaturated hydrocarbons (carbon chains)
2. Polycyclic aromatic hydrocarbons (PAHs)
3. Fullerenes and their derivatives

4. Porphyrins
5. Other unspecified organics

The first two classes have been studied extensively in the laboratory setting, and therefore, will be reviewed here.

1.3.1 Carbon Chains and the DIBs

Carbon chains have been cited as promising candidates for DIB carriers for many years [36, 37]. Their conjugated systems of electrons produce intense $\pi - \pi^*$ transitions at visible and UV wavelengths. Both the electronic oscillator strengths and dipole moments of (apolar) carbon chains increase with chain length, a fact that has enabled the detection of quite long chains – up to HC_{11}N and C_8H – in dark molecular clouds by radio astronomy methods [38, 39]. Laboratory spectra of carbon chains have been measured in microwave [40–42], visible, and UV [43–47] wavelength ranges. Such studies culminated in measurements of the electronic absorption spectra of carbon chain anions C_6^- , C_7^- , C_8^- and C_9^- , whose $\pi - \pi^*$ transitions were found to be very close to a number of DIBs [48, 49]. More detailed astronomical spectroscopy failed to yield a definite assignment of any DIBs to carbon chain anions [50–52], but even so, it is not possible to completely rule out carbon chains as potential DIB carriers – especially large chains where very strong excited state (S_n , $n \geq 2$) bands move into the visible [53].

1.3.2 PAHs and the DIBs

PAHs are good candidates for DIB carriers. They are thought to be present in a large number of environments in the ISM from the widespread detection of the UIRs. While the UIRs provide important constraints on the *type* of material responsible for the emission, they

are sufficiently broad and entangled that the identification of specific molecular species is not possible. These bands are believed to be emitted by large, internally excited molecules, and the only way to efficiently generate such excitation is through the absorption of visible or UV photons. The first electronic transitions of small, multi-ring neutral PAHs lie in the near-UV. For example, the $S_1 \leftarrow S_0$ transition for anthracene occurs at 361.17 nm, and that for pyrene at 367.43 nm. A PAH molecule needs to have at least 25 – 30 carbon atoms to absorb strongly in the visible range, and the number of carbon atoms must be significantly larger in order to achieve absorption in the red and near IR parts of the spectrum where many DIBs are located.

On the other hand, even small PAH cations absorb visible and near-IR photons. For example, the $D_2 \leftarrow D_0$ transitions of the naphthalene and phenanthrene cations lie at 670.65 nm and 891.90 nm, respectively; the $D_3 \leftarrow D_0$ transition of the naphthalene cation has been measured to be 454.85 nm. The ionization energies of PAHs are below 9.3 eV, and for PAHs with more than two aromatic rings they are less than 7.9 eV. Neutral PAHs should therefore be ionized rapidly in the regions of the ISM exposed to UV radiation, i.e., close to stars or in diffuse interstellar clouds.

A few attempts have been made to compare PAH electronic spectra with the DIBs [54–56], but while there are some close coincidences, no DIBs have been found to have an exact match with the measured electronic transitions of neutral PAHs or their cations. In general, if PAHs are indeed DIB carriers, one might expect them to be responsible for the wider DIB features due to their large sizes as compared to the molecules detected by high resolution spectroscopy.

In the past, the lack of laboratory data for PAHs led to a suite of extensive studies in matrices [56–59], helium droplets [60, 61] and the gas phase (both isolated [61–69] and in

clusters [69–74]). There are, however, several experimental challenges that make it difficult to obtain the spectra of cold, isolated, multi-ring PAHs which could be directly compared with the DIBs.

In the gas phase, it is hard to achieve high PAH concentrations due to the low vapor pressure of the solid. For example, most PAH samples have to be heated to high temperatures, sometimes in excess of 300 – 500 °C, in order to carry out direct absorption studies or to efficiently seed them into molecular beams. The heated vapor is vibrationally hot, which in turn, leads to significant spectral broadening. Furthermore, PAH cations are usually created in some form of a discharge which leads to even broader spectra, thanks to the high electron temperature in such sources.

To alleviate some of these concerns, the spectra of clusters of small PAHs with argon atoms have been recorded [69–74]. Cluster dissociation has been especially useful in obtaining the spectra of cold PAH cations with rare gases [71–74]. Here, neutral PAH clusters were threshold photoionized to yield the PAH⁺-Rg species. In principle, both vibrational and electronic spectra of PAH cations can be obtained in this fashion, but the spectra acquired are shifted from that of bare chromophore, sometimes by 100 – 200 cm⁻¹ – thus, precluding a direct comparison to the DIBs or the UIR features.

Similar studies of PAHs in argon and neon matrices conducted at cryogenic temperatures suffer from similar limitations. The PAH concentration can be varied as they are deposited into a matrix and as a result, very good signal-to-noise ratios can be obtained with a relatively simple apparatus. The main problems with PAH spectra in matrices are the spectral shift and the broadening due to interactions with matrix atoms, but such data sets form an excellent overview from which to select candidate molecules for more detailed study.

1.4 Protonated PAHs

1.4.1 Protonated PAHs in ISM

Neutral PAHs in the ISM may be ionized by UV radiation. The PAH cations created may react with highly abundant hydrogen to form protonated PAHs. In order to pursue quantitative chemical modeling, the reaction rates between hydrogen and PAH cations, dehydrogenated cations, and protonated PAHs were measured in flowing afterglow-selected ion flow tube experiments for benzene, naphthalene and pyrene [75]. No significant reactions were observed between PAH cations or protonated PAHs with H_2 molecules, but PAH cations reacted with atomic hydrogen at nearly the Langevin rate ($\sim 10^{-10} \text{ cm}^3/\text{s}$) to form protonated PAHs. Dehydrogenated PAH cations associated with H atoms at almost the same rate. On the other hand, the association of protonated PAHs with atomic hydrogen was found to be ≥ 100 times slower. This led authors to conclude that protonated PAHs would be a dominant form of PAHs in ISM regions with a high ionization rate and hydrogen atom abundance such as diffuse or translucent clouds.

Based on these experiments, the interstellar chemistry involving benzene/naphthalene cations and hydrogen atoms have been considered [76]. It was concluded that even at low densities, the radiative association with H is very efficient, and that the H_2 molecule loss dissociation channel for protonated species is not likely to be important in these reactions.

Another source of protonated PAHs in the denser regions of the ISM may be the proton transfer from known protonated species such as H_3^+ , HCO^+ , H_3O^+ [77–81], to neutral PAHs. Reaction rate studies of proton transfer to a range of organic compounds in a recent flowing afterglow-selected ion flow tube experiment [82] found that the proton transfer to alkanes, alkenes and alkynes was dissociative, non-dissociative or both, depending on whether the

proton donor was H_3^+ , H_3O^+ or N_2H^+ , respectively. Aromatic hydrocarbons, on the other hand, underwent only non-dissociative proton transfer, forming protonated PAHs.

To extend such laboratory results on a few selected species to the more general population of potential DIB and UIR carriers in the ISM, a statistical theory has been developed to consider the hydrogenation and charge states of PAHs in diffuse interstellar clouds [83,84]. The main result was that small PAHs, specifically those with less than 20 carbon atoms, would be destroyed by the interstellar UV radiation field; intermediate size PAHs with 20 – 30 carbon atoms would be highly dehydrogenated but stable; and large PAHs would be nearly fully hydrogenated, and even protonated. In terms of the overall charge balance, large PAHs were predicted to be essentially 100% ionized, with 60 – 80% of intermediate size PAHs estimated to be in their cationic or protonated forms.

Both of the experiments outlined above indicate that protonated PAHs should exist in the ISM, especially for large, multi-ring PAHs. Smaller PAHs should exist in a wide range of hydrogenation and charge states that depend sensitively on the H/H_2 ratio and the UV radiation flux. In particular, the photostability of each type of PAH will play an important role in the overall chemical speciation of the important suite of compounds.

1.4.2 Protonated PAHs and the DIBs

Protonated PAHs are closed-shell ions. Their electronic structure is closely related to that of neutral PAHs in that protonated PAHs retain a system of conjugated electrons which is responsible for the lowest energy $\pi - \pi^*$ electronic transitions. As described in Chapter 3, such transitions are expected to be red-shifted with respect to the same transition in the corresponding neutral PAH. The amount of this shift is not known, but from simple energetic considerations, it is expected to be on the order of a few tens of nanometers. Thus,

even small PAHs with only 3 – 4 aromatic rings may absorb in the DIB wavelength range.

1.4.3 Other Applications of Protonated Aromatics

Aromatic electrophilic substitution reactions are an important class of reactions in organic chemistry. Such substitution reactions occur in two steps:



where AH is a neutral aromatic molecule and E is an electrophilic reagent (Cl, Br, NO₃, SO₃H, etc.). Protonated aromatic molecules are believed to be intermediates in these aromatic electrophilic substitution reactions [85].

In living organisms, many molecules form hydrogen bonds. UV radiation may break some of these bonds and lead to the formation of protonated aromatic species. The study of protonated aromatics may help lead to a better understanding of the radiation damage processes that occur in biological cells.

1.4.4 Previous Studies of Protonated Aromatics

UV spectra of protonated aromatic compounds (carbonium ions) were studied in anhydrous solution with HF and BF₃ [86]. These spectra consisted of broad absorption bands and were located at visible wavelengths. To re-examine these results, solution spectra for the complexes of aromatic compounds with Al₂Br₆ and Al₂Cl₆ have been recorded [87]. When the C₆H₆·Al₂Br₆ complex was stabilized with HBr, protonated benzene was created. The UV spectrum of this solution displayed a broad structureless band with a maximum near 330 – 340 nm and another broad absorption feature at wavelengths shorter than 275 nm. A systematic study of UV, IR and NMR spectra of protonated aromatic compounds performed in similar solutions [88] found UV absorption band maxima at 332 nm for pro-

tonated benzene, 390 nm for protonated naphthalene, 408 nm for protonated anthracene, 510 nm for protonated phenanthrene, and 476 nm for protonated pyrene.

More directly relevant to the results presented in this thesis are the gas phase photodissociation spectra of organic compounds obtained in an ion cyclotron resonance mass spectrometer [89,90]. Among the experiments carried out was the UV photodissociation of protonated benzene. The recorded spectrum had two broad featureless absorption bands with maxima at 330 and 240 nm. These bands corresponded to the $S_1 \leftarrow S_0$ and $S_2 \leftarrow S_0$ electronic transitions of protonated benzene. The protonation led to relatively large redshifts: ~ 80 nm for the S_1 electronic state and $\sim 40 - 50$ nm for the S_2 state; the widths of the bands measured were $\sim 25 - 35$ nm FWHM. The spectrum was recorded with 10 nm resolution and most likely, the dissociation was multiphoton [91].

The structure of protonated benzene has been the subject of a number of theoretical studies [92–95]. Originally, σ - and π -complexes were considered as two possible structures. The proton binds to a carbon atom in the σ -complex forming a CH_2 site, while in the π -complex, the proton binds to the system of aromatic electrons. Later, the bridged structure in which the proton binds to the C–C bond was added for consideration. These studies have established that the σ -complex is a stable isomer of protonated benzene, the bridged structure is a first order transition state, and the π -complex is a second order transition state.

For larger systems, the structures and vibrational frequencies of protonated naphthalene, protonated pyrene, protonated coronene and protonated circumcoronene have been calculated using density functional theory [23]. All stable isomers were found to have σ -complex structures. Reactions of H atoms with PAH cations to form the protonated σ -complexes were found to be exothermic by 55 – 62 kcal/mol. The energies for both isomers and the

barrier height for 1–2 isomerization of protonated naphthalene have been calculated as well. The main goal of this study was to investigate vibrational spectra of protonated PAHs and, possibly, compare them with the UIRs.

Symmetric and asymmetric C–H stretching vibrations of the CH₂ site of protonated PAHs are characteristic of the σ -complex structure. The spectrum of these vibrations has been measured in gas phase IR dissociation experiments with clusters of protonated benzene with Ar, N₂, CH₄ and H₂O [3,96], an experiment that provided solid experimental proof that the σ -complex is the stable, lowest energy isomer of protonated benzene. The cluster experiment was promptly followed by the IR multiphoton dissociation spectroscopy of protonated benzene using free electron laser in the 6.2 – 9.3 μ m wavelength region [97].

1.5 Research Goals

The goal of this thesis is to study the gas phase properties of protonated PAHs and their interaction with visible and UV radiation. The purpose is to assess whether small protonated PAHs are an important component of ‘molecular grains’ in the ISM, and to investigate the relationship between protonated PAHs and the DIBs. Another outcome of the study would be a better understanding of intrinsic properties of protonated PAHs. There are two main questions addressed by the research presented here:

1. Do protonated PAHs exist in the interstellar medium?
2. Are protonated PAHs the carriers of the diffuse interstellar bands?

To date, only the low resolution spectrum of protonated benzene has been recorded in the gas phase. Electronic spectra of protonated polycyclic aromatic molecules with a few aromatic rings need to be recorded, and data obtained should be compared with the

observed DIBs. Photodissociation has been chosen as the method to record the spectra of protonated PAHs in this thesis, whose structure is described below.

Density functional theory calculations are performed in Chapter 2 in order to analyze the possible dissociation channels of protonated PAHs. In addition, the fate of protonated PAHs upon their recombination with electrons is investigated. Chapter 3 concentrates on the electronic structure of protonated PAHs and on predictions for the $S_1 \leftarrow S_0$ electronic transition wavelengths. A full compendium of the results from Chapters 2 and 3 is presented in Appendix A. The photostability of protonated PAHs is investigated in Chapter 5 via their photodissociation by visible and UV nanosecond lasers. The visible photodissociation spectrum of clusters of protonated anthracene with water is discussed in Chapter 6. The results are summarized in Chapter 7. Chapter 4 contains a detailed description of the experimental setup and some of its most important components. Draft drawings of the discharge parts and critical electric circuit diagrams are located in Appendix B. Appendix C contains the documentation for the data acquisition software developed in this thesis.